

Communication

Chlorido-pentamethylcyclopentadienyl-[2-(2-pyridyl-κN)-ferrocenyl-κC]-iridium(III)

Stefan Weigand and Karlheinz Sünkel * 

Department of Chemistry, Ludwig-Maximilians-University Munich, Butenandtstr. 5-13, 81377 Munich, Germany
* Correspondence: suenk@cup.uni-muenchen.de

Abstract: Treatment of 2-pyridyl-ferrocene with $[\text{Cp}^*\text{IrCl}_2]_2$ in the presence of NaOAc produces the title compound $\text{Cp}^*\text{ClIr}[(\text{C}_5\text{H}_3\text{C}_5\text{H}_4\text{N}-\kappa\text{N},\kappa\text{C})\text{Fe}(\text{C}_5\text{H}_5)]$ (**2**) in low yield. A crystal structure determination shows the (S_pS_{Ir}/R_pR_{Ir})-**2** enantiomeric pair of diastereomers.

Keywords: 2-pyridylmetallocenes; iridium half-sandwich complexes; cyclometallation; crystal structure determination

1. Introduction

Cyclometalated organometallic complexes have been intensively studied for a long time due to their potential applications in catalysis, anticancer therapy and luminescence. Particularly well studied were iridium half-sandwich complexes of the type “ $\text{Cp}^*\text{Ir}(\text{C}^X)\text{Y}$ ” [1–4] for the first two types of applications. However, despite the less pronounced luminescence properties of this compound type, some studies were also devoted to these possible applications [5,6]. A special subgroup of these compounds includes those where the C^N ligand is a 2-pyridyl-benzene derivative, which is π -coordinated via the benzene ring to a $\text{Cr}(\text{CO})_3$ or a cationic CpIr or CpRu fragment [7–9]. The main focus of these studies was the diastereoselectivity of the cyclometallation step, and numerous DFT studies on this particular topic were reported. One major result was that electrostatic repulsions determine the stereochemical outcome of these cycloiridation reactions. Another important group of organometallic compounds are donor-functionalised ferrocenes, which have been shown to have numerous applications mainly in the realms of catalysis and anticancer drug research [10–14]. Considering these overlapping applications, it seemed to be natural to combine these two research areas and study the heteronuclear $\text{Fe}(\text{II})$ - $\text{Ir}(\text{III})$ complexes involved [4,15–17]. In most cases, the ferrocene moiety was only present in the side-chain, in part due to the fact that in cyclometallation reactions, iridium apparently prefers cyclometallation of a phenyl group over a ferrocene group [18], or, even more unexpected, a metallocene-to-metallocene interconversion occurs [19]. Only rarely has cycloiridation occurred directly at the ferrocene cyclopentadienyl ring, leading to a complex showing both planar and metal-centred chirality [20]. Our group has shown in recent years that cyclometallation of 2-pyridyl-ferrocene is possible, and we obtained complexes with $\text{Pt}(\text{II})$ [21], $\text{Hg}(\text{II})$ [22] and very recently with $\text{Au}(\text{III})$ [23]. Here, we report our study on the cycloiridation of 2-pyridyl-ferrocene with $[\text{Cp}^*\text{IrCl}_2]_2$.

2. Results

2.1. Synthesis and Spectroscopic Characterisation

The reaction of 2-pyridyl-ferrocene **1** with $[\text{Cp}^*\text{IrCl}_2]_2$ ($\text{Cp}^* = \eta^5$ -pentamethylcyclopentadienyl), according to the general synthetic protocol for cycloiridations [24], yields a dark red coloured solution (Scheme 1). Chromatographic work-up on silica gel using a CH_2Cl_2 :EtOAc gradient elution gives three fractions. The first two weakly coloured fractions contain neither ferrocene- nor Cp^*Ir - attributable signals in their ^{13}C -NMR spectra and appear to contain the same compound of unknown structure (Figures S3 and S4). The third intensely red-coloured fraction shows in its ^1H - and ^{13}C -NMR spectra a relatively



Citation: Weigand, S.; Sünkel, K. Chlorido-pentamethylcyclopentadienyl-[2-(2-pyridyl-κN)-ferrocenyl-κC]-iridium(III). *Molbank* **2024**, *2024*, M1770. <https://doi.org/10.3390/M1770>

Academic Editor: Kristof Van Hecke

Received: 10 January 2024

Revised: 25 January 2024

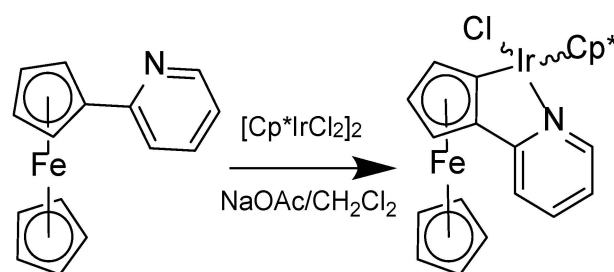
Accepted: 1 February 2024

Published: 2 February 2024



Copyright: © 2024 by the authors. Licensee MDPI, Basel, Switzerland. This article is an open access article distributed under the terms and conditions of the Creative Commons Attribution (CC BY) license (<https://creativecommons.org/licenses/by/4.0/>).

large number of signals attributable to 2-pyridyl-ferrocene and Cp*Ir fragments (Figures S5 and S6). It appears from the stronger (and sharper) signals in both ^1H and ^{13}C -NMR spectra that this fraction is still a mixture with unreacted starting material (for comparison, see Figures S1 and S2). The ^1H -NMR spectrum shows three groups of signals at $\delta = 8.7$ – 6.7 , 5.7 – 3.6 and 2.1 – 1.5 ppm, which integrate approximately 4:8:12, corresponding to $[\text{C}_5\text{H}_4\text{N}]$, $[\text{C}_5\text{H}_3 + \text{C}_5\text{H}_5]$ and $[\text{C}_5(\text{CH}_3)_5]$ protons (compound **1** has 4 phenyl, 9 cyclopentadienyl and no methyl protons; a cyclometalated product like **2** would have 4 phenyl, 8 cyclopentadienyl and 15 methyl protons. Thus, a content of ca. 20% residual **1** can be estimated. All these signals are broad without a fine structure. (It should be noted that similar broad signals were observed in the ^1H -NMR spectra of cycloiridated metallocenyloxazolines with a chloride ligand on iridium [15,25,26].) Since any structural assignment based on these NMR spectra appeared ambiguous, recrystallisation from CH_2Cl_2 / petroleum ether at -30°C was attempted. After standing for ca. 10 weeks, a few red crystals appeared, which were studied by X-ray crystallography and mass spectrometry. Both methods confirmed that this compound was the desired cycloiridated complex **2**. The yield was, however, very low and not sufficient for obtaining meaningful NMR spectra. Even after standing for several more months, no further crystals appeared.



Scheme 1. Synthesis of compound **2**.

2.2. Crystallographic Study

Compound **2** crystallises in the monoclinic centrosymmetric space group $C2/c$ with two independent molecules in the unit cell, together with CH_2Cl_2 and H_2O (Figure 1; lattice solvents not shown). Both molecules are more or less identical, showing only minor differences in the relative orientation of the ferrocene cyclopentadienyl rings (Figure S7). No higher crystallographic symmetry could be found, however. The cyclopentadienyl rings on iron have nearly the same distance from the metal, with a relative orientation intermediate between eclipsed and staggered. The substituted cyclopentadienyl ring, the pyridine ring and the chelate ring are close to coplanar (torsion angles C-C-C-N $10.3(7)/5.3(7)^\circ$ and Ir-C-C-C $13.6/6.5^\circ$).

Since $C2/c$ is a centrosymmetric space group, the crystals also contain the mirror-related (S_pS_{Ir})-**2** isomers. Important geometrical parameters are shown in Table 1.

Table 1. Important bond parameters in the crystal structure of **2** compared with two related structures from the literature.

Bond Length [\AA] and Angles [$^\circ$] ¹	Molecule A	Molecule B	LIZBAA ²	UJEKAX ³
Ir–Cl	2.411(2)	2.443(2)	2.426(1)	2.410(3)
Ir–N	2.110(5)	2.115(5)	2.220(4)	2.107(9)
Ir–C _{Fc}	2.042(5)	2.051(5)	2.038(5)	2.04(1)
Ir–CT _{cp*}	1.834(3)	1.822(3)	1.822	1.824
Fe–CT _{cp,sub}	1.664(3)	1.657(3)	1.649	1.656
Fe–CT _{C₅H₅}	1.656(4)	1.650(3)	1.644	1.658
C _{Fc} –Ir–N	77.6(2)	78.1(2)	76.9(2)	77.5(4)

Table 1. Cont.

Bond Length [Å] and Angles [°] ¹	Molecule A	Molecule B	LIZBAA ²	UJEKAX ³
C _{Fe} -CT _{cp,sub} -CT _{C5H5} -C'	13.1	21.1	10.3	17.3
Fe...Cl	4.036(2)	3.968(2)	3.850(1)	5.077(3)
Fe...Ir	3.901(1)	3.832(1)	3.8440(6)	3.820(2)

¹ CT are the centroids of the Cp rings: Cp*, C₅H₅ and Cp_{sub}. Substituted Cp ring of ferrocene. C_{Fe} is the ferrocene carbon atom bonded to iridium. C' is the carbon atom of the C₅H₅ ring closest to the projection of the C_{Fe}-CT_{cp,sub} vector onto the C₅H₅ ring. ² See ref. [22]. ³ See ref. [17].

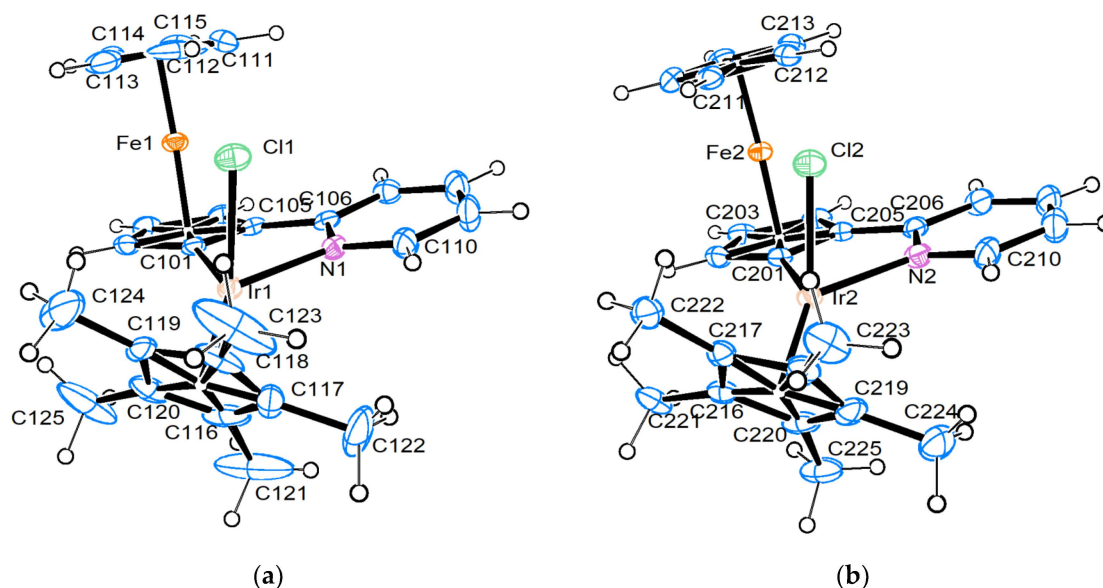
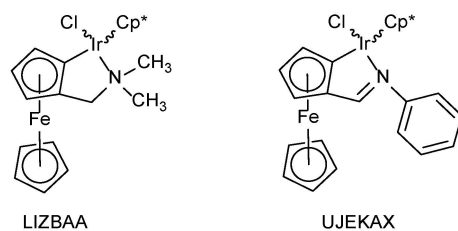


Figure 1. (a) Molecular structure of molecule A of compound **2**; the (*R_pR_r*) diastereomer is shown; (b) molecular structure of molecule B of compound **2**; the (*R_pR_r*) diastereomer is shown. Thermal ellipsoids are drawn at the 30% probability level.

A look at the Cambridge Structural Database (accessed on 6 January 2024) shows 343 hits for the search term “Cp*Ir(C‘N)X”, of which only six contain ferrocene units in general but only 2 (LIZBAA and UJEKAX), contain a cyclometalated ferrocene. LIZBAA contains a 1-dimethylaminoethyl substituent and UJEKAX contains a phenylimino substituent on the ferrocene part (see Scheme 2). The former shows the same (*S_pS_r*) diastereomer as compound **2**, with the chloride substituent directing towards the ferrocene unit (“small” Fe...Cl distance), while the latter contains the (*S_pR_r*) diastereomer (“large” Fe...Cl distance). However, most of the other metrical parameters of **2** are more similar to the phenylimino derivative UJEKAX.



Scheme 2. Structures of LIZBAA and UJEKAX.

3. Discussion

As had been observed with several iron- or cobalt-complexed cyclopentadienyl oxazolines before when using NaOAc as base for the cycloiridation [17,23], the reaction of **1**

with $[\text{Cp}^*\text{IrCl}_2]_2$ led to the recovery of the starting material and only the partial formation of the desired iridicyclic 2. The X-ray analysis of the crystals obtained after prolonged standing contain the $(S_pS_{Ir}/R_pR_{Ir'})$ enantiomeric pair of diastereomers. This contrasts with the observation that cycloiridation of phenyliminoferrocene yields the $(R_pS_{Ir}/S_pR_{Ir'})$ diastereomers [17]. A computational study related to the latter compound showed that the $(R_pR_{Ir'}/S_pS_{Ir})$ diastereomer would be ca. 2 kcal/mol more stable than the actually structurally characterised product, and it was concluded that the product formation was not under thermodynamic control. The result of this computational study is also in sharp contrast with the computations related to the $\text{Cr}(\text{CO})_3$ -coordinated cycloiridated phenylpyridines, where it was found that the *syn*-chloro isomers (as found in our structure of compound 2) are 7–8 kcal/mol less stable than their *trans* counterparts [7]. The fact that in our compound 2, as well as in structurally related compounds containing a $\text{Cp}^*\text{IrCl}(\text{C}^{\wedge}\text{N})$ unit, the ^1H -NMR signals were very broad might be regarded as a sign of stereochemical lability with dynamic dissociation of the chloride ligand, although other explanations are possible as well. Our crystals appeared only after prolonged standing, and only in very low yield, which excluded further characterisation by NMR methods, and thus no comparison with the original mixture is possible. In particular, we cannot even say if the compound found in the crystal structure corresponds to the “observed” signals of the ^{13}C -NMR spectrum. Therefore, we feel that unfortunately nothing can be said about the stereoselectivity of this particular cyclometallation reaction. The “pitfalls” in the discussion of stereoselectivity in the formation of planar-chiral metallacycles has been discussed in depth [27].

4. Materials and Methods

4.1. General Remarks

The starting material (2-pyridyl)-ferrocene 1 was prepared as described by us before [28]. All other solvents and reagents were obtained from Aldrich and used as received. NMR spectra were measured on a JEOL ECP-270 instrument, using CD_2Cl_2 as solvent. Spectra were referenced against the residual solvent signals. Mass spectra were obtained on Finnigan MAT 90 and JEOL Mstation 700 instruments in DEI mode. Chromatographic separations were performed in Schlenk glass frits of ca. 20 mm diameter with a filling height of ca. 15 cm of silica gel, which had been suspended in petroleum ether. A slight overpressure of argon was used to promote the migration of the bands through the column.

NMR data of 1: ^1H -NMR (270 MHz, CDCl_3): δ = 8.50 (m, 1H), 7.58 (m, 1H), 7.42 (m, 1H), 7.07 (m, 1H), 4.92 (m, 2H), 4.40 (m, 2H), 4.05 (s, 5H). ^{13}C -NMR (101 MHz, CDCl_3): δ = 159.4, 149.4, 136.0, 120.5, 120.2, 83.8, 69.9, 69.7, 67.3.

4.2. Synthesis

Chlorido-pentamethylcyclopentadienyl-[2-(2-pyridyl- κN)-ferrocenyl- κC]-iridium(III) (2)

A solution of $[\text{Cp}^*\text{IrCl}_2]_2$ (0.25 g, 0.31 mmol), $\text{NaOAc}\cdot 3\text{H}_2\text{O}$ (0.090 g, 0.66 mmol) and 1 (0.17 g, 0.65 mmol) in CH_2Cl_2 (10 mL) was stirred for 20 h at room temperature. Then, the mixture was filtered through Celite and the solvent was evaporated completely in vacuo. The residue was taken up in the minimum amount of petroleum ether (PE) and placed on top of a silica gel chromatography column. Elution was tried first with PE, then PE/ CH_2Cl_2 1:1 and then pure CH_2Cl_2 , apparently without success. A 1:1 CH_2Cl_2 /EtOAc mixture eluted a faint yellow first fraction and a 1:2 CH_2Cl_2 /EtOAc mixture eluted a weak red second fraction. Finally, pure EtOAc eluted an intensely red third fraction. All three fractions were evaporated and examined by NMR spectroscopy. The first two apparently contained no ferrocene species (Figures S3 and S4). The third fraction contained, according to ^1H - and ^{13}C -NMR spectra, a mixture of at least two compounds contaminated by some unidentified impurities. It was therefore taken up in a CH_2Cl_2 /PE mixture and stored in a freezer at -30°C . After ca. 10 weeks, a few red crystals appeared, which were examined by X-ray crystallography and mass spectrometry.

$^1\text{H-NMR}$ (270 MHz, CD_2Cl_2 ; Figure S5): $\delta = 8.7\text{--}8.1$, $7.7\text{--}6.7$ (several multiplets, 4H, pyridyl protons), $5.6\text{--}3.6$ (several broad signals, 8 H, cyclopentadienyl protons), 1.73 (s)/1.62 s, (Cp^* protons).

$^{13}\text{C-NMR}$ (68 MHz, CD_2Cl_2 , Figure S6): “Major” compound (stronger signals, presumably **1**): $\delta = 159.5$, 149.6 , 136.2 , 120.8 , 120.3 ($\text{C}_5\text{H}_4\text{N}$), 84.2 , 70.2 , 67.6 ($\text{C}_5\text{H}_3\text{XY}$), 69.9 (C_5H_5); “minor” compound (weaker signals, presumably **2**): $\delta = 169.8$, 151.4 , 137.3 , 119.8 , 119.3 ($\text{C}_5\text{H}_4\text{N}$), 96.2 , 90.8 , 72.0 , 71.0 , 63.8 ($\text{C}_5\text{H}_3\text{XY}$), 88.3 (C_5Me_5), 69.8 (C_5H_5), 9.1 (C_5Me_5). [Assignments were based on comparisons with literature data.] There are also several other very weak signals, that might belong to a third species.

MS (DEI^+): $m/z = 624.9$ (M^+), 589.9 ($\text{M}^+ - \text{Cl}$), 469.0 ($\text{M}^+ - \text{Cl} - \text{FeC}_5\text{H}_5$), 263.0 ($\text{M}^+ - \text{IrCp}^*\text{Cl}$).

4.3. Crystal Structure Determination

The crystal was measured on a BRUKER KAPPA CCD system. The experimental details of the structure determinations are collected in Table S1 of the Supplementary Materials. The software package WINGX [29] was used for structure solution (SIR97), refinement (SHELXL 2018/3) [30], evaluation (PLATON) and graphical representation (ORTEP3 and MERCURY). Carbon bound hydrogen atoms were treated with a riding model, using the AFIX command of SHELXL.

5. Conclusions

We showed that cycloiridation of 2-pyridyl-ferrocene is possible, albeit in low yield, and no clear information on the diastereoselectivity of this reaction could be obtained. Further studies would be necessary concerning optimisation of yields and also on the influence of substituents both on the ferrocene and the pyridine moiety on the stereochemical outcome of the reaction.

Supplementary Materials: The following supporting information can be downloaded online: Figure S1: $^1\text{H-NMR}$ spectrum of compound **1**; Figure S2: $^{13}\text{C}\{^1\text{H}\}$ -NMR spectrum of compound **1**; Figure S3: $^{13}\text{C}\{^1\text{H}\}$ -NMR spectrum of fraction 1; Figure S4: $^{13}\text{C}\{^1\text{H}\}$ -NMR spectrum of fraction 2; Figure S5: $^1\text{H-NMR}$ spectrum of fraction 1; Figure S6: $^{13}\text{C}\{^1\text{H}\}$ -NMR spectrum of fraction 1; Figure S7: PLATON “AutoMolFit” projection of the two independent molecules of compound **2**. Table S1: Experimental Details of the Crystal Structure Determination.

Author Contributions: Conceptualisation, S.W. and K.S.; methodology, S.W.; validation, S.W. and K.S.; investigation, S.W.; writing—original draft preparation, S.W.; writing—review and editing, K.S.; visualization, K.S.; supervision, K.S.; project administration, K.S. All authors have read and agreed to the published version of the manuscript.

Funding: This research received no external funding.

Data Availability Statement: CCDC 2324126 contains the supplementary crystallographic data for this paper. These data can be obtained free of charge via www.ccdc.cam.ac.uk/data_request/cif (accessed on 6 January 2024) by emailing data_request@ccdc.cam.ac.uk or by contacting The Cambridge Crystallographic Data Centre, 12, Union Road, Cambridge CB2 1EZ, UK; fax: +44 1223336033.

Acknowledgments: We want to express our special thanks to I-P. Lorenz for providing us with the lab space for the herein described experiments. We are also grateful to P. Mayer for performing the X-ray data collection.

Conflicts of Interest: The authors declare no conflicts of interest.

References

1. Liu, Z.; Sadler, P.J. Organoiridium Complexes: Anticancer Agents and Catalysts. *Accounts Chem. Res.* **2014**, *47*, 1174–1185. [[CrossRef](#)] [[PubMed](#)]
2. Zhang, P.; Sadler, P.J. Redox-Active Metal Complexes for Anticancer Therapy. *Eur. J. Inorg. Chem.* **2017**, *2017*, 1541–1548. [[CrossRef](#)]
3. Li, X.; Ouyang, W.; Nie, J.; Chen, Q.; Huo, Y. Recent Development on $\text{Cp}^*\text{Ir(III)}$ -Catalyzed C–H Bond Functionalization. *ChemCatChem* **2020**, *12*, 2358–2384. [[CrossRef](#)]

4. Chen, Z.; Kacmaz, A.; Xiao, J. Recent Development in the Synthesis and Catalytic Application of Iridacycles. *Chem. Rec.* **2021**, *21*, 1506–1534. [[CrossRef](#)] [[PubMed](#)]
5. Deaton, J.C.; Taliaferro, C.M.; Pitman, C.L.; Czerwiec, R.; Jakubikova, E.; Miller, A.J.M.; Castellano, F.N. Excited-State Switching between Ligand-Centered and Charge Transfer Modulated by Metal–Carbon Bonds in Cyclopentadienyl Iridium Complexes. *Inorg. Chem.* **2018**, *57*, 15445–15461. [[CrossRef](#)]
6. Wang, L.; Liu, X.; Wu, Y.; He, X.; Guo, X.; Gao, W.; Tan, L.; Yuan, X.-A.; Liu, J.; Liu, Z. In Vitro and In Vivo Antitumor Assay of Mitochondrially Targeted Fluorescent Half-Sandwich Iridium(III) Pyridine Complexes. *Inorg. Chem.* **2023**, *62*, 3395–3408. [[CrossRef](#)]
7. Scheeren, C.; Maasarani, F.; Hijazi, A.; Djukic, J.-P.; Pfeffer, M.; Zaric, S.D.; LeGoff, X.-F.; Ricard, L. Stereoselective „Electrophilic“ Cyclometalation of Planar-Prochiral (η^6 -Arene)tricarbonylchromium Complexes with Asymmetric Metal Centers: Pseudo-T-4 [Cp*RhCl₂]₂ and [Cp*IrCl₂]₂. *Organometallics* **2007**, *26*, 3336–3345. [[CrossRef](#)]
8. Djukic, J.-P.; Boulho, C.; Sredojevic, D.; Scheeren, C.; Zaric, S.; Ricard, L.; Pfeffer, M. The Stereospecific Ligand Exchange at a Pseudo-Benzylic T-4 Iridium Centre in Planar-Chiral Cycloiridium (η^6 -Arene)tricarbonylchromium Complexes. *Chem. A Eur. J.* **2009**, *15*, 10830–10842. [[CrossRef](#)]
9. Djukic, J.-P.; Iali, W.; Pfeffer, M.; LeGoff, X.-F. Synthesis of Planar Chiral Iridacycles by Cationic Metal π -Coordination: Facial Selectivity, and Conformational and Stereochemical Consequences. *Chem. Eur. J.* **2012**, *18*, 6063–6078. [[CrossRef](#)]
10. Rauf, U.; Shabir, G.; Bukhari, S.; Albericio, F.; Saeed, A. Contemporary Developments in Ferrocene Chemistry: Physical, Chemical, Biological and Industrial Aspects. *Molecules* **2023**, *28*, 5765. [[CrossRef](#)]
11. Dwadnia, N.; Roger, J.; Pirio, N.; Cattey, H.; Hierso, J.-C. Input of P, N-(phosphanyl, amino)-ferrocene hybrid derivatives in late transition metals catalysis. *Coord. Chem. Rev.* **2018**, *355*, 74–100. [[CrossRef](#)]
12. Ornelas, C.; Astruc, D. Ferrocene-Based Drugs, Delivery Nanomaterials and Fenton Mechanism: State of the Art, Recent Developments and Prospects. *Pharmaceutics* **2023**, *15*, 2044. [[CrossRef](#)]
13. Ludwig, B.S.; Correia, J.D.; Kühn, F.E. Ferrocene derivatives as anti-infective agents. *Coord. Chem. Rev.* **2019**, *396*, 22–48. [[CrossRef](#)]
14. Dai, L.; Xu, D.; Yang, M.-J. Synthesis of 2-oxazoline ferrocenes: Towards high-efficient chiral ligands and catalysis. *J. Organomet. Chem.* **2023**, *999*, 122831. [[CrossRef](#)]
15. Liu, X.; Lv, A.; Zhang, P.; Chang, J.; Dong, R.; Liu, M.; Liu, J.; Huang, X.; Yuan, X.-A.; Liu, Z. The anticancer application of half-sandwich iridium(III) ferrocene-thiosemicarbazide Schiff base complexes. *Dalton Trans.* **2023**, *53*, 552–563. [[CrossRef](#)]
16. Shao, M.; Liu, X.; Sun, Y.; Dou, S.; Chen, Q.; Yuan, X.-A.; Tian, L.; Liu, Z. Preparation and the anticancer mechanism of configuration-controlled Fe(II)–Ir(III) heteronuclear metal complexes. *Dalton Trans.* **2020**, *49*, 12599–12609. [[CrossRef](#)] [[PubMed](#)]
17. Ge, X.; Chen, S.; Liu, X.; Wang, Q.; Gao, L.; Zhao, C.; Zhang, L.; Shao, M.; Yuan, X.-A.; Tian, L.; et al. Ferrocene-Appended Iridium(III) Complexes: Configuration Regulation, Anticancer Application, and Mechanism Research. *Inorg. Chem.* **2019**, *58*, 14175–14184. [[CrossRef](#)] [[PubMed](#)]
18. Arthurs, R.A.; Horton, P.N.; Coles, S.J.; Richards, C.J. Phenyl vs. Ferrocenyl Cyclometallation Selectivity: Diastereoselective Synthesis of an Enantiopure Iridacycle. *Eur. J. Inorg. Chem.* **2016**, *2017*, 229–232. [[CrossRef](#)]
19. Arthurs, R.A.; Horton, P.N.; Coles, S.J.; Richards, C.J. Metallocene to metallocene conversion. Synthesis of an oxazoline-substituted pentamethyliridocenium cation from a ferrocenyloxazoline. *Chem. Commun.* **2016**, *52*, 7024–7027. [[CrossRef](#)] [[PubMed](#)]
20. Arthurs, R.A.; Ismail, M.; Prior, C.C.; Oganessian, V.S.; Coles, S.J.; Richards, C.J. Enantiopure Ferrocene-Based Planar-Chiral Iridacycles: Stereospecific Control of Iridium-Centered Chirality. *Chem. Eur. J.* **2016**, *22*, 3065–3072. [[CrossRef](#)] [[PubMed](#)]
21. Sünkel, K.; Branzan, R.; Weigand, S. 2-Pyridylmetallocenes, part IV. Cycloplatination of 2-pyridyl-ferrocene, -ruthenocene and -cymantrene. Molecular structures of σ -Pt[CpM(C₅H₃(2-C₅H₄N))]Cl (DMSO) (M = Fe, Ru) and σ -Pt[CpFe(C₅H₃(2-C₅H₄N))](acac). *Inorg. Chim. Acta* **2013**, *399*, 193–199. [[CrossRef](#)]
22. Sünkel, K.; Weigand, S. 2-Pyridylmetallocenes: Part 3 [1]. Cyclomercuration of 2-pyridyl-ferrocene and 1-(2-pyridyl)-2-methyl-ferrocene. Molecular structures of [1-(2-C₅H₄N)-2-(CH₃)C₅H₃]Fe(C₅H₅), [1-(ClHg)-2-(2-C₅H₄N)C₅H₃]Fe(C₅H₅) and [1-(ClHg)-2-(2-C₅H₄N)-3-(CH₃)C₅H₂]Fe(C₅H₅). *Polyhedron* **2012**, *44*, 133–137. [[CrossRef](#)]
23. Weigand, S.; Sünkel, K. 2-Pyridylmetallocenes, Part VII. Synthesis and Reactivity of cycloaurated Pyridylmetallocenes: Spectroscopic and Crystallographic Characterization. *Z. Anorg. Allg. Chem.* **2024**. *submitted*.
24. Han, Y.-F.; Jin, G.-X. Cyclometalated [Cp*M(C⁺X)] (M = Ir, Rh; X = N, C, O, P) complexes. *Chem. Soc. Rev.* **2014**, *43*, 2799–2823. [[CrossRef](#)]
25. Arthurs, R.A.; Hughes, D.L.; Horton, P.N.; Coles, S.J.; Richards, C.J. Application of Transmetalation to the Synthesis of Planar Chiral and Chiral-at-Metal Iridacycles. *Organometallics* **2019**, *38*, 1099–1107. [[CrossRef](#)]
26. Arthurs, R.A.; Prior, C.C.; Hughes, D.L.; Oganessian, V.S.; Richards, C.J. Enantiopure Planar Chiral and Chiral-at-Metal Iridacycles Derived from Bulky Cobalt Sandwich Complexes. *Organometallics* **2018**, *37*, 4204–4212. [[CrossRef](#)]
27. Djukic, J.-P.; Hijazi, A.; Flack, H.D.; Bernardinelli, G. Non-racemic (scalemic) planar-chiral five-membered metallacycles: Routes, means, and pitfalls in their synthesis and characterization. *Chem. Soc. Rev.* **2007**, *37*, 406–425. [[CrossRef](#)] [[PubMed](#)]
28. Sünkel, K.; Weigand, S. 2-Pyridylmetallocenes: Part I. Electrophilic halogenation of 2-pyridylferrocene. Molecular structures of 2-pyridylferrocene and its a-brominated and-fluorinated derivatives. Synthesis of 2-pyridylruthenocene and 2-pyridylcymantrene. *Inorg. Chim. Acta* **2011**, *370*, 224–229. [[CrossRef](#)]

-
29. Farrugia, L.J. WINGX and ORTEP for Windows: An update. *J. Appl. Cryst.* **2012**, *45*, 849–854. [[CrossRef](#)]
 30. Sheldrick, G.M. Crystal structure refinement with SHELXL. *Acta Crystallogr. Sect. C Struct. Chem.* **2015**, *71*, 3–8. [[CrossRef](#)] [[PubMed](#)]

Disclaimer/Publisher's Note: The statements, opinions and data contained in all publications are solely those of the individual author(s) and contributor(s) and not of MDPI and/or the editor(s). MDPI and/or the editor(s) disclaim responsibility for any injury to people or property resulting from any ideas, methods, instructions or products referred to in the content.